

Bethel University

Spark

Chemistry Faculty Publications

Chemistry Department

Winter 2021

Computational Analysis Beyond the Monomer Frontier Orbitals for Photovoltaic Donor-Polymer Candidates

Mitchell E. Lahm
Bethel University

Megan M. Niblock
Bethel University


John M. Migliore
Bethel University

Kendra M. Mckenzie
Bethel University

Hans P. Lüthi

See next page for additional authors

Follow this and additional works at: <https://spark.bethel.edu/chemistry-faculty>

 Part of the [Chemistry Commons](#)

Recommended Citation

Lahm, Mitchell E.; Niblock, Megan M.; Migliore, John M.; Mckenzie, Kendra M.; Lüthi, Hans P.; and King, Rollin A., "Computational Analysis Beyond the Monomer Frontier Orbitals for Photovoltaic Donor-Polymer Candidates" (2021). *Chemistry Faculty Publications*. 31.
<https://spark.bethel.edu/chemistry-faculty/31>

This Article is brought to you for free and open access by the Chemistry Department at Spark. It has been accepted for inclusion in Chemistry Faculty Publications by an authorized administrator of Spark.

Authors

Mitchell E. Lahm, Megan M. Niblock, John M. Migliore, Kendra M. Mckenzie, Hans P. Lüthi, and Rollin A. King

COMPUTATIONAL ANALYSIS BEYOND THE MONOMER FRONTIER ORBITALS FOR PHOTOVOLTAIC DONOR-POLYMER CANDIDATES

Mitchell E. Lahm^{*a}, Megan M. Niblock^{*a}, John M. Migliore^{*a}, Kendra D. McKenzie^{*a}, Hans P. Lüthi^b, Rollin A. King^{a,†}

^aDepartment of Chemistry, Bethel University, St. Paul, Minnesota

^bDepartment of Chemistry and Applied Biosciences, ETH Zürich, Zurich, Switzerland

Abstract

Scharber *et al.* proposed an efficiency model for organic photovoltaic cells based on the orbital energies of the monomers of the donor- and acceptor-polymers [Advanced Materials 18 (2006) 789–794]. We report theoretical extensions of this approach. First, the frontier-orbital energies and electronic spectra of *n*-length oligomers (*n* = 1 – 5) of 3-butylthiophene have been determined. The results show reasonable convergence with respect to system size at the point of a trimer with alkyl end caps. The HOMO-LUMO gap well matches computed excitation energies. Second, the structures and electronic spectra of dimers formed by three different monomers, with various linkages were determined. The electronic spectra of the dimers was computed as a function of the dihedral angle between the monomers to explore the response to geometrical distortion. Finally, for each of the top 21 monomer candidates provided by the Harvard Clean Energy Project, we have computed the excitation spectrum and constructed a frequency-dependent external quantum efficiency function. Inclusion of this additional information into the efficiency model gives a broad range of results. Further experiments are needed to determine if this straightforward extension of Scharber's model is worth the additional computational expense in the quest for practical, efficient donor-polymers.

†Corresponding author: rking@bethel.edu

Keywords: photovoltaic, organic, donor, excitation, Scharber, efficiency

Introduction

The search for more efficient and cost-effective photovoltaic cells has led, among several lines of inquiry, to the investigation of organic- and perovskite-based cells [1]. Specifically, bulk heterojunction organic cells hold the promise of less expensive and more environmentally friendly energy production [2–4]. In a typical such cell, a potential difference is created by the transfer of excited electrons from “donor” polymers to fullerene-based “acceptor” polymers which have been blended together [5]. A common such acceptor is a polymer of phenyl-C61-butyric acid methyl ester (PCBM, see Fig.1), although several other acceptors have been tested [6]. Meanwhile, a wide variety of donor polymers are being vigorously investigated.

The power conversion efficiency (PCE) of a cell is the percentage of input energy transformed into usable output energy. By 2011, organic solar cells with PCE's as high as 7% had been

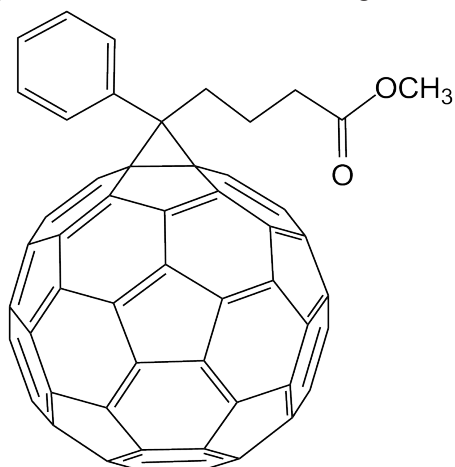


Figure. 1 Phenyl-C61-butyric acid methyl ester (PCBM), a common electron-acceptor.

reported [7–11] with estimates of the performance of future PCE's ranging from 8-11% [12–14]. Many recent theoretical studies have sought to discover or optimize donor molecules leading to improved conversion efficiency [15–19]. In 2017, Zanlorenzi *et al.* [20] reported finding numerous donor-acceptor pairs that have theoretical efficiencies of 9-10%. A parallel track of investigation has focused on how charge transfer might be facilitated by quantum coherence, including a search for lessons that might be learned from studying natural photosynthesis [21–24]. For example, Ari *et al.* [25] explored phthalocyanines, which resemble photosynthetic chromophores, as solar cell materials. Recently, Meng *et al.* [26] reported an experimental PCE of 17.3% in a tandem cell combining novel chromophore and electron-acceptors. Yost *et al.* explored the potential of triplet excitons which can support long diffusion lengths in organic semiconductors [27]. As a variety of promising approaches continue to be explored, the PCE will be joined by material durability and synthetic feasibility as decisive factors for widespread application.

In 2006, Scharber *et al.* [12] presented a theoretical model (hereafter referred to as “AM2006”) for estimating PCE in organic solar cells based only on frontier orbital energies. The model may be summarized by the following formula for PCE and the estimates used for its component factors. The PCE is expressed as

$$\text{PCE} = \frac{V_{OC} J_{SC} FF}{P_{in}} \quad (1)$$

which involves the open-circuit voltage (V_{OC}), the short-circuit density (J_{SC}), and the fill factor (FF). The FF accounts for the inability to simultaneously achieve maximum voltage and current. AM2006 sets both the FF as well as the maximum quantum efficiency (see Eqn. 3 below) to 0.65 [28, 29]. The input power P_{in} in Eqn. 1 is set to 1000 W/m², as the total average power density from a reference solar spectrum. We have used the ASTM G173-03 Reference Spectrum in this work [30].

The short-circuit density J_{SC} may be determined by integrating the product of the external quantum efficiency (EQE) and the number of incoming photons over a frequency range,

$$J_{SC} = \int EQE(\omega) * \#photons(\omega) d\omega \quad (2)$$

where in AM2006, the EQE is given by

$$EQE(\omega) = \begin{cases} 0.65, & \text{if } \hbar\omega > E_{opt} \\ 0, & \text{if } \hbar\omega < E_{opt} \end{cases} \quad (3)$$

where E_{opt} , the optical bandgap, is estimated by the magnitude of the HOMO-LUMO gap of the absorbing donor monomer. AM2006 requires no excited-state computations on the monomer, at the cost of only a crude estimate of excitation energy and the incorporation of no other molecule-specific spectroscopic information.

Alharbi *et al.* [31] presented an enhanced model incorporating the absorption spectrum to account for frequency-dependent absorption (as well as the diffusion length to account for the relative probability of charge transport versus recombination). Using experimentally determined absorption spectra, the authors demonstrated that accounting for frequency-dependence can substantially change the predicted J_{SC} and therefore the relative efficiency. Alharbi *et al.* suggested that a corresponding computational approach is possible, which we have pursued in this work.

The V_{OC} is generally the electrical potential difference between the cathode and anode when the circuit is disconnected. AM2006 estimates the V_{OC} as follows

$$V_{OC} = LUMO_{acceptor} - HOMO_{donor} - 0.3 \text{ eV} \quad (4)$$

where the 0.3 eV is an empirical loss factor. Another commonly imposed criterion is that the donor LUMO is at least 0.3 eV higher than the acceptor LUMO. Otherwise, the electron transfer from the donor to the acceptor may be inefficient. Within the AM2006 model, a balance is needed, where the acceptor LUMO is low enough to promote charge transport, but also as high as possible to maximize the potential difference with the donor HOMO. The initial AM2006 model used a LUMO acceptor value for PCBM of -4.3 eV. Beyond monomer screening, Vandewal *et al.* [32] explored the nature of the polymer-fullerene open-circuit voltage, emphasizing the need to account for their interaction in the most rigorous approaches. The significance of interfacial excited states was explored by Few *et al.* [33].

Experiments support the conclusion that hot charge-transfer states may also form so that any surplus energy carried over by the electron may not all be wasted [34, 35]. Given the approximations (including the neglect of bulk effects) made by AM2006 and similar models, they are not expected to quantitatively predict PCE's. They are successful if they can direct further investigation by identifying monomers most likely to form efficient cells. In 2016, Scharber [36] reported the results of experiments on 8 polymers with PCE's of 3.3-6.5% and fill factors of 60-71%, concluding that AM2006 is quite applicable to understanding their performance. This model imposes a theoretical upper limit of about 13% efficiency.

Tortorella *et al.* [37] investigated theoretical screening of benzofulvene derivatives for use in organic solar cells, demonstrating that good results could be obtained using B3LYP

to predict molecular structures and orbital energies. The valuable work by Bérubé, Gosselin, Gaudreau and Côté [13] calibrated the AM2006 model by comparing density functional theory (DFT) and experimental results for 30 donor polymers, paired with fullerene-based acceptors. The authors derived corrections to DFT (specifically B3LYP [38, 39]) orbital energies to optimize the fit to experimental cyclic voltammetry and cell efficiency measurements. They found that "the EQE is the main problem of Scharber's model". The use of a constant FF was shown to be less significant. In the present work, we have utilized the orbital energy corrections developed by Berube *et al.*, and we have also theoretically explored a more sophisticated EQE.

The Harvard Clean Energy Project (HCEP) applied a customized version of the AM2006 model to automatically generated donor monomers [40, 41]. The HCEP stochastically generated 2.3 million candidates built from 26 small, building-block fragments. These fragments were mostly mono- and bi-cyclic chromophores, some containing sulfur, selenium, or silicon. (Li *et al.* [42] provide an analysis of some new donor monomers that aid in the ranking of such 100 building blocks.) The HCEP employed a number of computational tactics to allow for robust automation, such as averaging orbital energies computed by several different density functionals. These molecules were then ranked by their predicted PCE. The structures of the top 21 donor candidates (as of 2015) were provided for further investigation (see Fig. 2).

We explore three extensions of the AM2006 model in this work. First, for 3-butylthiophene, we compute HOMO/LUMO and excitation energies as a function of polymer length for $n = 1 - 5$ to gauge the limitation of computations on only a single monomer. Second, we have explored the structure and electronic excited states for dimers of three of the top candidates. The geometries and relative energies of dimers formed from various chemical linkages are compared. We also report the electronic absorption spectra of the dimers as a function of the connecting dihedral angle between the virtually planar monomers. Finally, for each of the 21 top candidates we have computed the lowest singlet electronic excitation energies and oscillator strengths, and have used this information to construct frequency-dependent, molecule-specific EQE functions. We then determined the resulting PCE's. Of

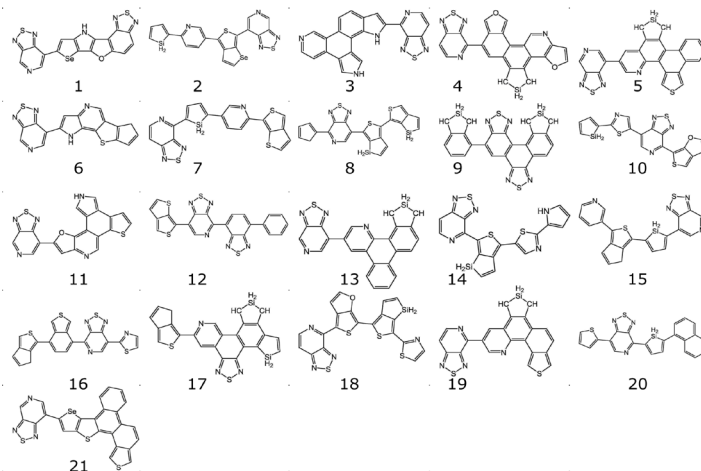


Figure 2. The top 21 candidates by PCE as of 2015 produced by a stochastic and AM2006-model-based search by the Harvard Clean Energy Project. We have arbitrarily numbered them.

particular interest is whether the *relative* PCE's are significantly changed by the incorporation of spectral data. If the more intricate models distinguish between candidates with roughly equal PCE's according to AM2006, then the additional computational effort will be justified. In neither case are bulk effects accounted for, but theoretical molecule-specific EQE's may provide more precise guidance for further research.

Methods

The structures, relative energies, and HOMO energy levels for 3-butylthiophene monomer up to its corresponding pentamer were determined using a 6-31G** basis set [43–47] and the B3LYP [38, 39] density functional implemented in the QChem4 program [48]. We note Bérubé *et al.* [13] applied an extended, periodic model of the donor, but this is often not done, and it was not done in the HCEP search. For the analysis of the dimers of the electron-donor candidates, the Gaussian03 package [49] was used first to optimize the structures at the 6-31G* B3LYP level. Electronic excited-state energies and oscillator strengths of the dimer configurations were computed using the QChem4 package to apply TD-DFT using the BHHLYP density functional [50] with a 6-31+G* [51] basis set. Subsequently on the dimers, the same methods were used to perform constrained optimization at various, fixed dihedral angles followed by excited-state TD-DFT computations.

The ground-state geometrical structures of the top 21 monomer candidates were used as provided by the HCEP. The corresponding orbital energies were computed using B3LYP and the 6-311++G(2d) [47, 52, 53] basis set. Predicting the relative performance of the HCEP candidates is of primary significance in this work. However to check the reasonableness of the absolute PCEs predicted, we have also performed the same analysis of three monomers from the paper by Bérubé *et al.* [13] for which the experimental PCE is known. The monomers P8, P9, and P10 from that paper were optimized using B3LYP and the 6-311G(2d) basis set, and then investigated using the same approaches as the HCEP candidates, described below.

The five lowest singlet excited-state energies and oscillator strengths were determined by TD-DFT using the BHHLYP density functional and the 6-31+G* basis set. This spectral data was used to construct the model EQE's. Two functional forms were assumed for the bandwidths, Gaussian and Lorentzian. Letting E_i and f_i represent the energy and oscillator strength, respectively, of the i 'th singlet excited state, the model EQE's can be expressed as follows.

$$\text{G-EQE} = \sum_i^5 f_i \frac{1}{\sigma\sqrt{2\pi}} e^{-(E-E_i)^2/(2\sigma^2)} \quad (5)$$

$$\text{L-EQE} = \sum_i^5 f_i \frac{\Gamma}{2\pi} \frac{1}{(E-E_i)^2 + (\frac{\Gamma}{2})^2} \quad (6)$$

The value of $\Gamma = 0.75\text{eV}$ for the Lorentzian model was set arbitrarily. The value of σ was chosen so that the Gaussian full-width at half-maximum would match that of the Lorentzian function. Since only relative performance is in view, we have normalized the computed oscillator strengths by dividing by the largest computed oscillator strength in the HCEP set of 21 molecules to represent the unitless

absorption probability. This maximum value obtained in any of the EQE spectra was that for candidate 7, and accordingly the Gaussian and Lorentzian models were scaled by 0.952 and 0.903, respectively. Experimenting with different choices of linewidths and scaling was found not to drastically impact the relative values of the predicted PCE's.

However, carrying out the same analysis using B3LYP as the density functional in the TD-DFT computations was found to produce unrealistically high PCE's due to B3LYP's tendency to predict excitation energies that are too low. With the BHHLYP functional, the relative ordering of the PCEs remained similar, but with more reasonable absolute values as well.

In order to compute the final efficiencies, an estimate of V_{oc} is needed. Lacking another ready alternative, we have retained the Bérubé-modification of the AM2006 formula for the V_{oc} from the energies of the donor HOMO (the B3LYP value) and the acceptor LUMO (-4.23 eV). Many preliminary optimizations were performed with PM3 [54]. The HOMO and LUMO images presented for two of the monomers were computed with 6-31G*B3LYP and using Spartan16 [55].

Results and Discussion

Oligomers of 3-butylthiophene

The structure of 3-butylthiophene (BTP) polymers is shown in Fig. 3. Table 1 shows the 6-31G** B3LYP HOMO and LUMO energy eigenvalues of oligomers of BTP of length 1-5, and also the energies for the oligomers with methyl and ethyl terminal groups. As the chain lengthens, the HOMO approaches a value near that of -5.05 eV obtained by others [12]. Of interest here is how large of a system must be evaluated to approach the polymeric limit, or at least to present a more robust value for use in a model which uses orbital energies.

Meier [56] comprehensively reviewed the impact of chain length in conjugated oligomers involving electron donors and acceptors, showing that oligomers of electron donors typically have excitation energies that approach the polymeric limit exponentially. More recently, Varkey *et al.* [57] reported a computational study focused on the impact of donor-acceptor functionalization on the properties of π -conjugated oligomers, including polyacetylenes, polynes, and polythiophenes. They reported exponential convergence toward the long-chain limit of most structural and molecular properties (with the exception being the hyperpolarizability). Among these properties, the HOMO energy and first absorption frequency converge more rapidly than others analyzed in that work (e.g., bond alternation). Meier provided specific examples of oligomers whose long-wavelength absorptions converged rapidly to within about 0.2 eV of the long-

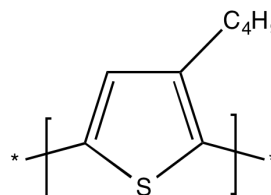


Figure 3. The 3-butylthiophene oligomer.

chain limit at the trimer length.

From a practical perspective, it is helpful to know the minimum-sized computation that can provide a HOMO acceptably close to the polymeric limit for use in a simple model. Here, we see that replacing the terminal hydrogens with methyl groups significantly speeds convergence with respect to the number of monomers. There is limited advantage to using the larger ethyl groups. We note that Yu *et al.* [15] have also investigated dimers of donor candidates.

Turan *et al.* [58] reported B3LYP computations on 80 different push-pull organic chromophores which possess donor-acceptor and donor-thiophene-acceptor-thiophene motifs. Their results favor tetrameric oligomers, where feasible, as the optimal chain length at which to determine properties such as orbital energies. Clearly, computational cost is also a consideration when screening a large number of monomers, or monomers of larger size. Also, one must consider the overall accuracy of the PCE model when determining if longer oligomers are worth the effort.

The excitation energy approximated as the energy difference between the HOMO and LUMO is a principal input of the AM2006 model of PCE, so it is noteworthy that the orbital energy gaps reported in Table 1 are in excellent agreement with the substantially more computationally costly 6-31+G* BHHLYP excitation energies from TD-DFT computations.

Conformations and Spectra of Dimers

Three monomers were chosen from the list of top candidates provided by the HCEP [40]. For variety, we chose one containing silicon (I), one containing selenium and silicon (III), and one containing neither of these (II). The three monomers are depicted in Fig. 4.

The connection points on the monomers indicated in Fig. 4 were selected for analysis because the analogous sites on molecular fragments were used as bonding sites by the HCEP in

Table 1: Orbital and excitation energies for oligomers of 3-butylthiophene of length *N* with given terminal groups.^a

N	HOMO(eV)	LUMO(eV)	Δ (LUMO-HOMO)	S_1 (eV)	S_1 (osc.)
-H					
1	-6.15	-0.11	6.04	5.81	0.099
2	-5.52	-0.87	4.65	4.55	0.402
3	-5.22	-1.20	4.03	4.11	0.863
4	-5.09	-1.39	3.70	3.79	1.181
5	-5.03	-1.47	3.56	3.65	1.388
-CH₃					
1	-5.66	0.03	5.69	5.39	0.135
2	-5.31	-0.71	4.60	4.58	0.523
3	-5.01	-1.17	3.84	3.96	0.926
4	-5.06	-1.22	3.84	3.88	1.122
5	-4.98	-1.39	3.59	3.75	1.321
-CH₂CH₃					
1	-5.63	0.00	5.63	5.49	0.171
2	-5.20	-0.76	4.44	4.47	0.600
3	-5.06	-1.14	3.92	3.99	0.948
4	-4.95	-1.33	3.62	3.68	1.228
5	-4.90	-1.44	3.46	3.56	1.431

^aThe geometrical structures were optimized using B3LYP with a 6-31G** basis set. The orbital energies are those from 6-31G** B3LYP. The S_1 excitation energy and oscillator strength were computed using TD-DFT and the BHHLYP functional with a 6-31+G** basis.

the construction of the candidates. We first examined the relative energies of the various dimer minima that might be formed by connections at these selected points. The relative energies of the resulting optimized dimer structures are given in Table 2, along with the value of the dihedral angle between the monomers. In all three monomers, the **A** site is located off of a thiadiazole-pyridine bicycle. However, sites **B** and **C** substantially differ chemically one candidate to another.

For all three dimers, the lowest-energy isomer results from connecting at point **A** of each monomer. In a polymer, other connectivities would be necessary for chain-building, and kinetic factors would be important as well as thermodynamic ones. On the thermodynamic side, for dimer I bonding at site **A** with **B** results in a dimer I(**A-B**) that is only 0.3 kcal mol⁻¹ higher in energy. (Connecting site **B** with **B** gives dimer I(**B-B**) which is 2.5 kcal mol⁻¹ higher.) Thus, the synthesis of an **A-B** connected polymer looks reasonable. For the isomers of dimer II, the results are analogous but now the II(**A-B**) dimer is 5.3 kcal mol⁻¹ above II(**A-A**). For the isomers of dimer III, the **A-B** and **A-C** linkages are competitive, and the III(**A-B**) and III(**A-C**) dimers lay 3.3 and 2.3 kcal mol⁻¹, respectively, above the III(**A-A**) isomer.

The excitation energies and oscillator strengths for these dimer minima are provided in Table 3. The absorption properties are seen to vary significantly between the isomers, with some similarities. For all three dimers, the greatest oscillator strength corresponds with the S_1 state of the dimer formed from **A-A** linkage. However, several of the other structures, including all of the mixed (**A-B** and **A-C**) dimers, also have significant oscillator strengths for excitation to the S_2 state. All can contribute to the overall probability of excitation, and therefore to the quantum efficiency.

The dihedral angles for each dimer minimum are included in Table 2. The non-planarity of the dimers and the potential

Table 2: Relative energies^a for differently connected dimers^b of monomer candidates I, II, and III.

Dimer	dihedral angle ^c	Energy (kcal/mol)	Dimer	dihedral angle	Energy (kcal/mol)	Dimer	dihedral angle	Energy (kcal/mol)
I			II			III		
A-A	145.3	0.00	A-A	145.9	0.00	A-A	-153.7	0.00
A-B	39.2	0.32	A-B	102.5	5.34	A-B	45.7	3.30
B-B	-102.6	2.50	B-B	94.7	9.27	A-C	-130.3	2.32
						B-B	130.8	7.00
						B-C	62.9	7.15
						C-C	-101.1	7.76

^aVibrationless 6-31G* B3LYP relative energies.

^bThe two monomers were linked at the given letter designations, which are illustrated in Fig. 4.

^cDihedral angle centered on the bond linking the monomers; precise definition given with structures in SI.

Table 3: Excitation energies in eV (with oscillator strengths immediately below)^a for the lowest singlet excited states of differently connected dimers^b of monomer candidates I, II, and III.

I	S_1	S_2	S_3	II	S_1	S_2	S_3	III	S_1	S_2	S_3
A-A	2.52	2.61	2.91	A-A	2.23	2.60	3.10	A-A	2.01	2.54	2.94
	1.2E+00	5.3E-02	6.5E-03		1.6E+00	3.9E-04	6.4E-05		1.7E+00	2.8E-02	1.5E-03
A-B	2.50	2.69	2.75	A-B	2.66	2.74	2.89	A-B	2.37	2.56	2.71
	8.4E-01	1.9E-01	2.0E-02		7.2E-01	2.9E-01	2.5E-02		4.7E-01	4.6E-01	4.3E-02
B-B	2.66	2.66	2.98	B-B	2.60	2.63	3.08	A-C	2.39	2.53	2.79
	3.7E-02	4.4E-01	1.1E-01		6.3E-01	1.4E-01	8.7E-04		7.9E-01	3.1E-01	3.4E-02
								B-B	2.51	2.55	3.24
									3.9E-01	3.5E-01	2.4E-03
								B-C	2.50	2.55	2.83
									3.3E-01	4.6E-01	3.0E-03
								C-C	2.51	2.54	3.27
									5.8E-01	3.8E-01	4.2E-01

^aProperties computed with TD-DFT using 6-31+G* BHHLYP (at 6-31G* B3LYP optimized geometries).

^bThe two monomers were linked at the given letter designations, which are illustrated in Fig. 4.

conformational requirements in a polymer or bulk environment raise the questions of stability and absorption properties of these dimers as a function of the dihedral angle connecting them. Thus, we have investigated the torsional potential of the seven lowest-energy dimers by repeated optimization using 6-31G* B3LYP at constrained values of the central dihedral angle. The resulting potential curves are shown in Fig. 5.

Although the minimum for dimer I(A-B) occurs at a dihedral angle of 39° , this dimer also has a low energy conformation at -150° and the nearby planar arrangement is only ~ 1 kcal mol $^{-1}$ above the global minimum. Dimer II(A-B) is seen to strongly prefer orthogonal arrangement, though ~ 1 kcal mol $^{-1}$ is enough energy to reach the range from roughly 60° to 120° , or from -60° to -120° .

The potential curves for dimers III(A-B) and III(A-C) are similar with minima at approximately -120° , and a very flat potentials between 40° and 150° , and from -50° to -150° . The primary difference is that the A-B linkage tolerates near planarity more easily with a planar peak at only 3.0 kcal mol $^{-1}$. The potential curves for the dimers using the same chemical linkage, I(A-A), II(A-A), and III(A-A), are quite similar with one crowded high-energy planar arrangement, and minima near the other planar arrangement. In conclusion, for the mixed-linkage dimers most relevant to polymers, dimer I(A-B) has a non-planar minimum but its planar conformation is only 1 kcal mol $^{-1}$ higher, while dimer II(A-B) strongly prefers an orthogonal arrangement. Both III(A-B) and III(A-C) have comparatively flat potential curves, with III(A-B) having the lowest energy at planarity.

Since the most promising configurations for use in solar cells appear to be I(A-B), III(A-B), and III(A-C), we have computed the excitation energies and oscillator strengths for the lowest excited singlet states of these three dimers as a function of the connecting dihedral angle. The results are illustrated in Fig. 6. Dimer I(A-B) is seen to have relatively uniform excitation energies as a function of dihedral angle, apart from its high-energy planar orientation. Its S_1 oscillator strength is large, peaking at 180° and decreasing

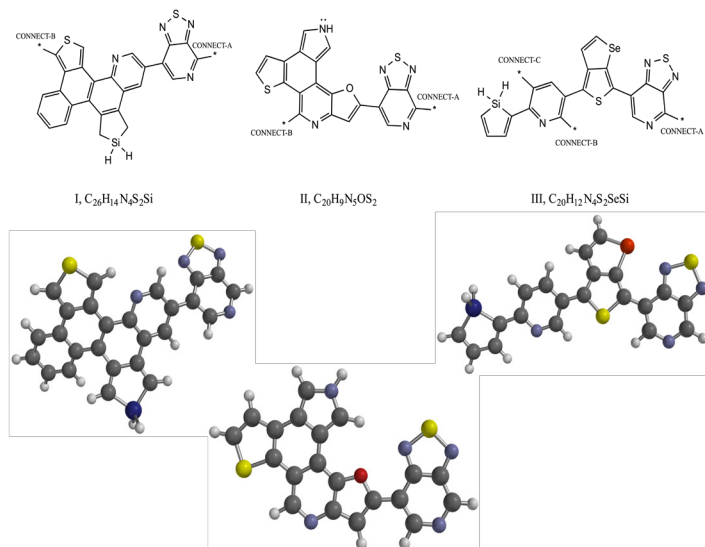


Figure 4. Structures of selected candidate monomers. These are monomers 5, 11, and 2, respectively in Fig. 2.

with deviation from planarity. Thus, a conformational twist in the polymer may lower the absorption probability significantly. The S_2 oscillator strength peaks at 0° , and could contribute modestly to absorption at larger dihedral angles, while the S_3 state is negligible.

For dimer III(A-B), the excitation energies are nearly uniform with respect to the dihedral angle. The oscillator strengths for the S_1 and S_2 states are very similar in magnitude in the low-energy range of the dihedral angle, and both would contribute substantially to absorption. For III(A-C), the results are similar in that the excitation energies depend little on the dihedral angle. In this case, the oscillator strength for the S_1 state is quite large, with the smaller S_2 state also having significant absorption potential. All three of these dimers, having significant oscillator strengths and low excitation energies at low-energy conformations of the dihedral angle appear worthy of further investigation. This kind

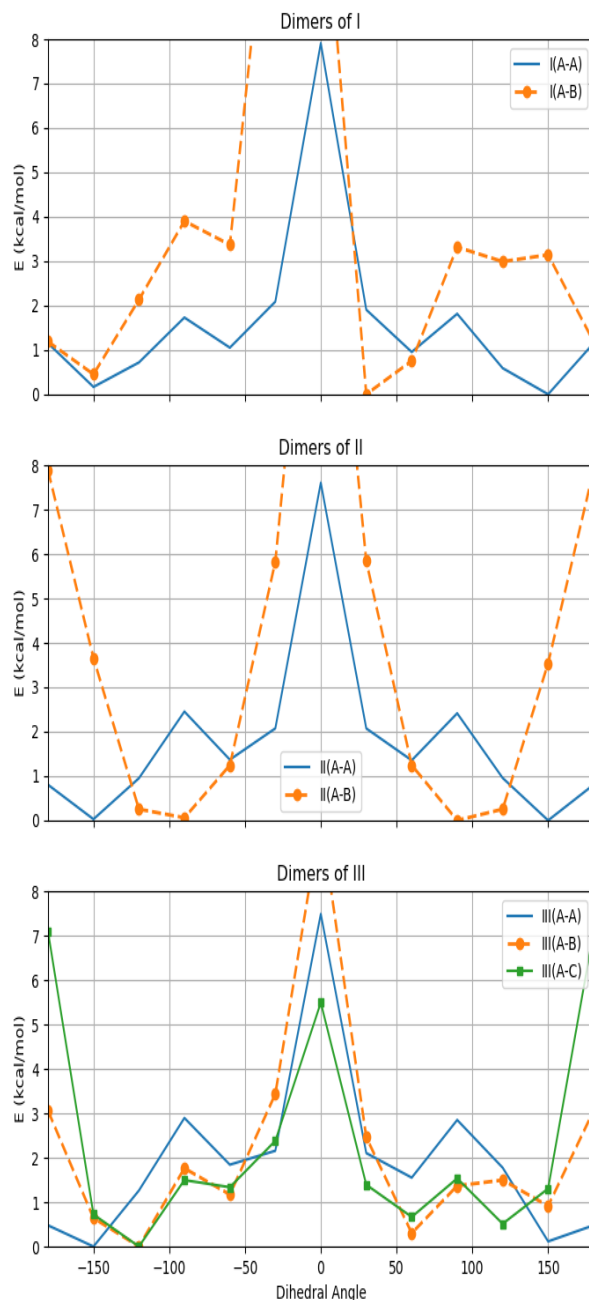


Figure 5. Ground-state potential energy of dimers as a function of the connecting dihedral angle, computed with 6-31G* B3LYP.

of computational analysis can contribute to the identification of promising donor polymers and the interpretation of the varying efficiencies obtained experimentally.

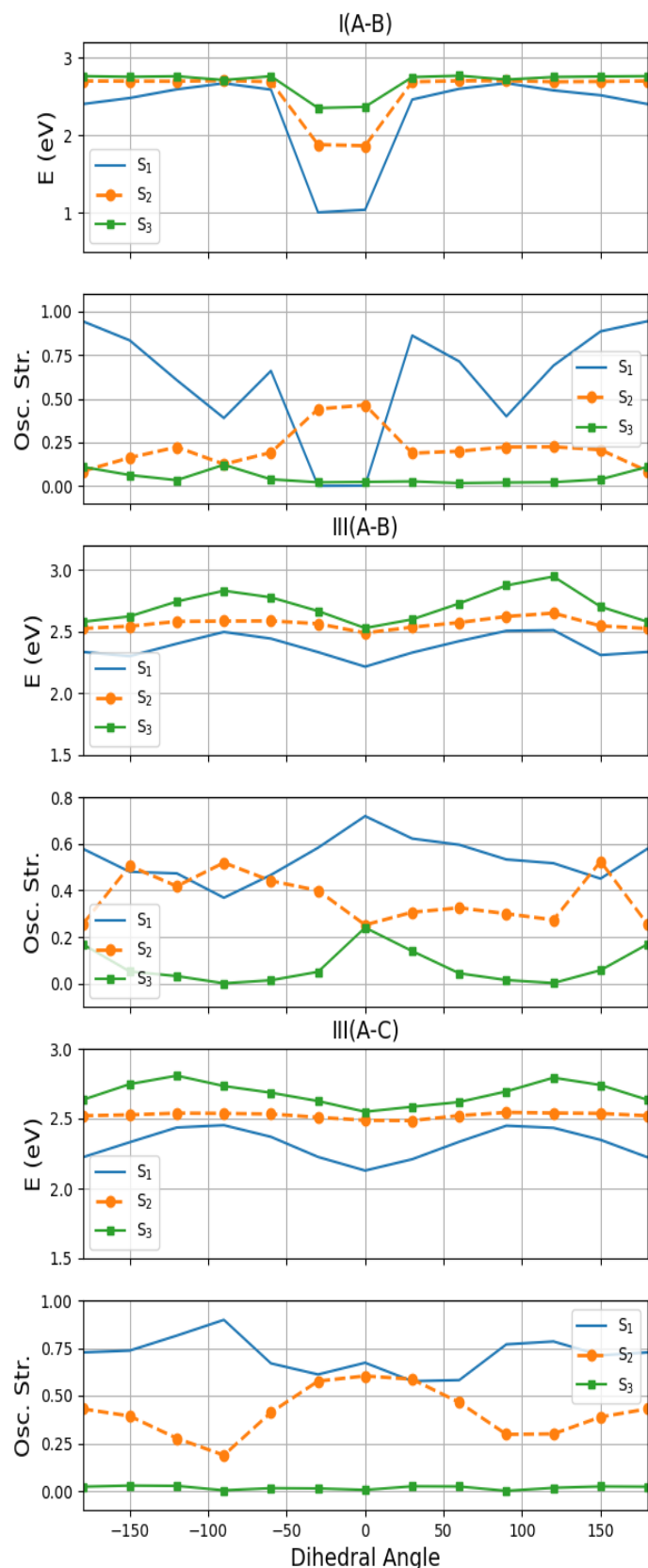


Figure 6. The lowest singlet excited-state energies and oscillator strengths computed by TD-DFT using 6-31+G* BHHLYP, at 6-31G* B3LYP constrained geometries.

Modelling the EQE with spectral data

The five lowest-energy singlet excited states for the top 21 candidates identified by the HCEP were computed using TD-DFT with the BHHLYP density functional and a 6-31+G* basis set, and are reported in Table 4. Model EQE curves were constructed from the excited-state data by the summation of both Gaussian- and Lorentzian-shaped peaks (see Methods). The resulting curves are illustrated in Fig. 7 for candidates 5 and 7. AM2006 estimates the optical gap as the HOMO-LUMO energy difference, and assigns a value of 0.65 to the EQE for all incident light of higher frequency. These particular candidates exemplify two extremes. Candidate 5 has low oscillator strengths for all excitations, while candidate 7 has a large oscillator strength for S_1 , as well as a significant one for S_2 .

The orbital plots shown in Fig. 8 demonstrate the reason underlying the two distinct cases. The HOMO and LUMO of candidate 5 have very little spatial overlap, resulting in a small oscillator strength. The LUMO in candidate 7 is similar, however, the presence of a silicon atom in the adjacent ring has the effect of extending both the HOMO and the LUMO onto this ring and into overlap with one another. Clearly, a model that includes only the orbital energies is incapable of describing these distinctions which manifest in transition dipoles and oscillator strengths.

These EQE models do not explicitly incorporate vibrational or bulk effects. Experimental absorption spectra indicate that actual absorption at high energies is not being captured by this model (see Fig. 4 of Alharbi *et al.* [31] and references there). However, the surface solar spectrum is less intense at higher energies, and the energy range of the computed excitations overlaps with the peak of the solar energy spectrum, suggesting that the efficiency models may be adequate for the estimation of total energy absorption.

In Table 5 we present the PCE's for all 21 candidates computed via 1) the AM2006 model with unadjusted B3LYP orbital energies; 2) the AM2006 model with the orbital energy corrections developed by Bérubé *et al.*[13]; 3) the G-EQE model; and 4) the L-EQE model. Several notable points are evident.

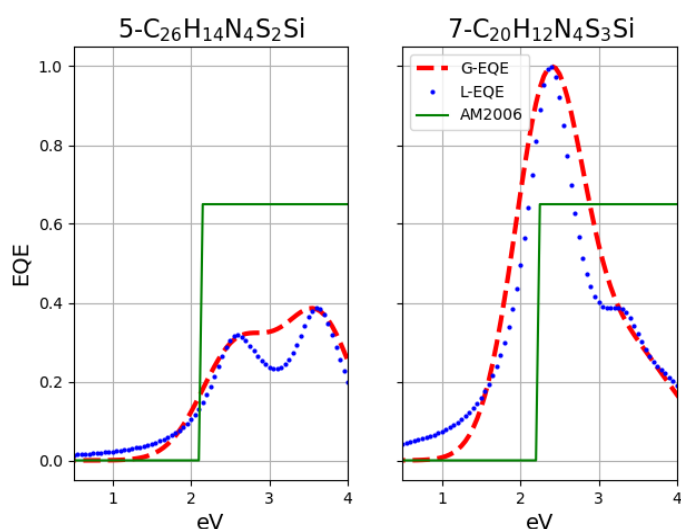


Figure 7. The external quantum efficiency (EQE) according to the AM2006 model (green solid), G-EQE (red dashed) and L-EQE (blue dots) models for HCEP candidates 5 (left) and 7 (right).

The 21 molecules were selected by the HCEP for high PCE's based on a composite of empirically-derived linear regressions of orbital energies computed with Hartree-Fock and 5 distinct density functionals. In addition, multiple conformers were examined, and the final values were determined by incorporating up to 75 distinct values. The top candidates examined here were selected from among millions tested as those having maximum PCEs by this particular metric [40, 41].

It is seen that without any empirical correction, the direct use of B3LYP energies gives PCE's that are too low at roughly 5%. The orbital-corrected values are narrowly ranged around 10%. Clearly by adjusting parameters, such as the acceptor LUMO or the linewidths used in the EQE models, the PCEs can be readily increased or decreased, but the main objective is to determine the relative performance.

Polymers of P8, P9, and P10 have experimentally produced

Table 4: The HOMO and LUMO energies, and the excitation energies (with oscillator strengths below) of the lowest singlet excited states of the HCEP candidate monomers.^a

Candidate	1	2	3	4	5	6	7
LUMO(eV)	-3.35	-3.32	-3.43	-3.35	-3.37	-3.27	-3.35
HOMO(eV)	-5.52	-5.44	-5.55	-5.47	-5.52	-5.52	-5.50
S ₁ (eV)	2.41	2.32	2.41	2.28	2.55	2.58	2.38
	0.669	0.564	0.414	0.413	0.268	0.435	1.027
S ₂ (eV)	2.92	3.10	2.88	2.72	2.87	3.78	3.32
	0.170	0.625	0.079	0.006	0.045	0.102	0.227
S ₃ (eV)	3.55	3.65	3.48	3.35	3.50	3.80	3.47
	0.012	0.070	0.020	0.021	0.023	0.388	0.013
S ₄ (eV)	3.89	3.84	4.00	3.63	3.60	4.01	3.92
	0.417	0.008	0.323	0.026	0.127	0.085	0.082
S ₅ (eV)	4.05	3.99	4.06	3.77	3.65	4.28	4.22
	0.118	0.011	0.008	0.331	0.228	0.031	0.020
Candidate	8	9	10	11	12	13	14
LUMO(eV)	-3.29	-3.32	-3.27	-3.35	-3.35	-3.35	-3.32
HOMO(eV)	-5.50	-5.55	-5.44	-5.50	-5.47	-5.50	-5.44
S ₁ (eV)	2.35	2.30	2.32	2.55	2.28	2.49	2.45
	0.647	0.219	0.799	0.364	0.732	0.199	0.630
S ₂ (eV)	3.31	2.57	3.15	3.24	3.15	2.91	3.36
	0.008	0.078	0.358	0.063	0.240	0.058	0.642
S ₃ (eV)	3.68	2.75	3.42	3.73	3.35	3.54	3.51
	0.346	0.001	0.058	0.372	0.018	0.184	0.104
S ₄ (eV)	3.78	2.84	3.89	3.78	3.83	3.75	3.68
	0.238	0.007	0.027	0.037	0.162	0.011	0.016
S ₅ (eV)	4.01	3.50	4.05	4.17	3.86	4.04	4.24
	0.009	0.027	0.192	0.048	0.020	0.135	0.001
Candidate	15	16	17	18	19	20	21
LUMO(eV)	-3.35	-3.29	-3.32	-3.32	-3.37	-3.35	-3.35
HOMO(eV)	-5.44	-5.52	-5.47	-5.44	-5.50	-5.42	-5.50
S ₁ (eV)	2.29	2.38	2.09	2.30	2.47	2.20	2.50
	0.730	0.515	0.248	0.865	0.343	0.829	0.596
S ₂ (eV)	3.06	3.32	3.04	3.28	2.94	3.11	3.26
	0.223	0.191	0.076	0.346	0.027	0.064	0.240
S ₃ (eV)	3.61	3.43	3.33	3.56	3.42	3.40	3.48
	0.032	0.234	0.157	0.084	0.039	0.169	0.027
S ₄ (eV)	3.92	3.60	3.73	3.80	3.53	3.94	3.59
	0.195	0.010	0.297	0.013	0.148	0.025	0.090
S ₅ (eV)	4.02	4.04	3.79	3.91	3.63	4.07	3.95
	0.096	0.028	0.007	0.109	0.151	0.001	0.017

^aThe structures were used as provided by the HCEP. The HOMO and LUMO eigenvalues were computed at the 6-311++G(2d) B3LYP level. The excited state energies and oscillator strengths were computed using TD-DFT with 6-31+G* BHHLYP.

PCE's of 4.0%, 4.7%, and 5.5%, respectively [13]. The L-EQE predicted PCE's are 9.4%, 6.8%, and 6.2%. It is unfortunately not possible to draw a correspondence between the small differences in the currently observed performance of these closely related polymers and differences predicted from their absorption spectra. From the simpler AM2006 and corrected AM2006 results reported here, one would also predict P8 to have the highest PCE, while

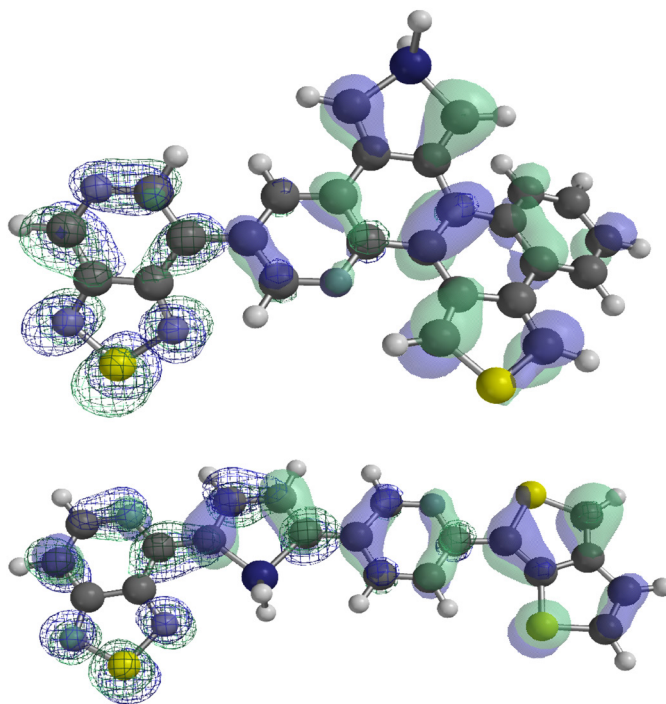


Figure 8. The LUMO (mesh) and HOMO (transparent) for candidates 5 (top) and 7 (bottom).

Table 5: Predicted power conversion efficiencies.

Density Functional Basis Set	AM2006 ^a	AM2006-Adj ^b	G-EQE	L-EQE
	B3LYP 6-311++G(2d)	B3LYP 6-311++G(2d)	TD-BHHLYP 6-31+G*	TD-BHHLYP 6-31+G*
7-C ₂₀ H ₁₂ N ₄ S ₃ Si	4.89	10.13	10.87	10.63
18-C ₂₀ H ₁₀ N ₄ OS ₄ Si	4.80	10.06	10.10	9.93
20-C ₂₃ H ₁₅ N ₃ S ₂ Si	5.00	10.40	10.09	9.46
10-C ₁₈ H ₁₀ N ₄ OS ₃ Si	4.42	9.58	9.50	9.46
12-C ₂₃ H ₁₁ N ₅ S ₄	4.95	10.24	9.15	8.92
15-C ₂₁ H ₁₄ N ₄ S ₂ Si	4.97	10.30	8.73	8.61
2-C ₂₀ H ₁₂ N ₄ S ₂ SeSi	4.80	10.06	8.17	8.30
1-C ₁₇ H ₆ N ₆ OS ₂ Se	4.85	10.07	7.73	8.03
8-C ₂₂ H ₁₅ N ₃ S ₃ Si ₂	4.53	9.65	7.30	7.47
14-C ₁₈ H ₁₁ N ₅ S ₃ Si	4.80	10.06	6.92	7.36
16-C ₂₃ H ₁₂ N ₄ S ₄	4.48	9.59	6.19	6.32
21-C ₂₅ H ₁₁ N ₃ S ₃ Se	4.89	10.13	5.93	6.14
4-C ₂₄ H ₁₂ N ₄ O ₂ SSi	4.95	10.24	4.80	4.82
3-C ₂₂ H ₁₂ N ₆ S	5.42	10.75	4.57	4.73
6-C ₁₇ H ₉ N ₅ S ₂	4.29	9.33	3.87	4.44
17-C ₂₄ H ₁₅ N ₃ S ₂ Si ₂	4.74	9.96	4.14	4.26
19-C ₂₂ H ₁₂ N ₄ S ₂ Si	5.11	10.41	3.59	3.83
11-C ₂₀ H ₉ N ₅ OS ₂	4.89	10.13	3.38	3.81
5-C ₂₆ H ₁₄ N ₄ S ₂ Si	5.04	10.30	2.84	3.21
9-C ₂₄ H ₁₄ N ₄ S ₂ Si ₂	4.61	9.74	3.13	2.98
13-C ₂₄ H ₁₄ N ₄ SSi	4.89	10.13	2.25	2.53
P8 ^c	2.60	7.44	9.30	9.43
P9 ^c	2.52	7.22	6.80	6.77
P10 ^c	2.34	6.84	6.03	6.17

^aCalculated from HOMO and LUMO energies [12].

^bIncorporating orbital energy corrections of Bérubé *et al.* [13].

^cMonomers included in Bérubé *et al.* [13].

with a slightly different approach to the orbital energies Bérubé *et al.* [13] calculated P9 to have the highest PCE.

The primary purpose here is to see if drastically different PCE's are predicted from the set of HCEP candidates. The relative PCE's predicted by the two frequency-dependent EQEs are quite similar, with the choice of Gaussian or Lorentzian lineshapes being unimportant. The ranking of the candidates by the L-EQE model is completely disparate from that of the AM2006 model. More relevantly, the molecule-specific, frequency-dependent G-EQE and L-EQE models predict a large variation in performance among the candidates. Monomer 7, for example, has a much higher predicted PCE than monomer 5, corresponding to their contrasting EQEs.

Alharbi *et al.* [31] presented collected experimental absorption spectra for seven materials used in excitonic cells in Fig. 4 of their paper. Strong fluctuations are present in these spectra including some wavelength ranges at which the absorption is near zero. This data suggests that the large variations and molecular-specific absorption features calculated here are also present at least to some extent in relatively thin layers of the bulk material. There is good reason to think that the wide variation in predicted performance is more realistic than the near-identical values provided by more limited models.

Consideration of the monomeric oscillator strengths dramatically changes the *a priori* expectations of the relative absorption properties of these polymers. Since the purpose of any of these models is not quantitative accuracy but to point toward candidates most worthy of experimental synthesis and testing, this is a significant conclusion. Finally, we note recent work on the potential to reach higher PCEs for semitransparent devices via an alternative EQE model [59].

Conclusion

Oligomers of 3-butylthiophene were explored to determine the sensitivity of the HOMO energy to chain length. It was found that even for such a small monomer, the value of the HOMO converges rapidly with respect to the number of monomer units. The results suggest that evaluating HOMO's for subunits larger than dimers or trimers is unnecessary, and also that the substitution of methyl groups in the terminal chain positions speeds convergence with respect to system size.

The dimers of three monomer candidates were investigated in detail. Some thermodynamically reasonable connection points were explored for each dimer. The ground-state potential energy curve, the lowest excitation energies, and the associated oscillator strengths were determined as a function of the inter-monomer dihedral angle. Two of the dimers investigated appear worthy of further study, combining low excitation energies with high oscillator strength near a preferred geometrical configuration.

The energies and oscillator strengths of the lowest singlet excited states of 21 monomer candidates were computed. Frequency-dependent external quantum efficiencies were modelled using this data. The resulting EQE's led to the prediction of a broad range of PCE values, even for a set of candidate monomers that had virtually the same PCE's according to only their orbital

energies. Although the PCE's computed with model EQE's will not be quantitatively accurate, they clearly distinguish between this set of otherwise comparable candidates. Further experimental work is necessary to establish the utility of this approach.

Acknowledgements

The authors thank the Harvard Clean Energy Project for making their top donor candidate molecular structures available. One of the authors (RAK) acknowledges the Minnesota Supercomputing Institute (MSI) at the University of Minnesota for computing time (URL: <http://www.msi.umn.edu>). One of the authors (HPL) acknowledges inspiring discussions with F. Alharbi and F. El-Mellouhi of the Qatar Energy and Environment Research Institute (QEERI) in Doha.

References

- [1] Yan, J.; Saunders, B. R. *RSC Adv.* **2014**, *4*, 43286–43314.
- [2] Brédas, J.-L.; Norton, J. E.; Cornil, J.; Coropceanu, V. *Accounts of Chemical Research* **2009**, *42*, 1691–1699.
- [3] Heeger, A. In *Global Sustainability: a Nobel Cause*; Schellhuber, H. J., Molina, M., Stern, N., Huber, V., Kadner, S., Eds.; Cambridge University Press: UK, 2010; Chapter 23, pp 271–280.
- [4] Scharber, M. C.; Sariciftci, N. S. *Progress in polymer science* **2013**, *38*, 1929–1940.
- [5] Wang, Y.; Wei, W.; Liu, X.; Gu, Y. *Sol. Energy Mater. Sol. Cells* **2012**, *98*, 129–145.
- [6] Mahdaviifar, Z.; Salmanizadeh, H. *J. of Photochem. and Photo-bio. A: Chemistry* **2015**, *310*, 9–25.
- [7] Liang, Y.; Xu, Z.; Xia, J.; Tsai, S.-T.; Wu, Y.; Li, G.; Ray, C.; Yu, L. *Adv. Mat.* **2010**, *22*, E135–E138.
- [8] Liang, Y.; Yu, L. *Acc. Chem. Res.* **2010**, *43*, 1227–1236.
- [9] Chu, T.-Y.; Lu, J.; Beaupré, S.; Zhang, Y.; Pouliot, J.-R.; Wakim, S.; Zhou, J.; Leclerc, M.; Li, Z.; Ding, J. *J. Am. Chem. Soc.* **2011**, *133*, 4250–4253.
- [10] Price, S. C.; Stuart, A. C.; Yang, L.; Zhou, H.; You, W. *J. Am. Chem. Soc.* **2011**, *133*, 4625–4631.
- [11] He, Z.; Zhong, C.; Huang, X.; Wong, W.-Y.; Wu, H.; Chen, L.; Su, S.; Cao, Y. *Adv Mater* **2011**, *23*, 4636–4643.
- [12] Scharber, M. C.; Mühlbacher, D.; Kop, M.; Denk, P.; Waldauf, C.; Hegger, A. J.; Braber, C. *J. Adv. Mat.* **2006**, *18*, 789–794.
- [13] Bérubé, N.; Gosselin, V.; Gaudreau, J.; Côté, M. *J. Phys. Chem. C* **2013**, *117*, 7964–7972.
- [14] Zhang, L.; Yu, M.; Peng, Q.; Zhao, H.; Gao, J. *Mol. Sim.* **2016**, *42*, 47–55.
- [15] Yu, M.; Zhang, L.; Peng, Q.; Zhao, H.; Gao, J. *Comp. and Theor. Chem.* **2015**, *1055*, 88–93.
- [16] Liu, X.; He, R.; Shen, W.; Li, M. *J. of Power Sources* **2014**, *245*, 217–223.
- [17] Liu, X.; Li, M.; He, R.; Shen, W. *Phys. Chem. Chem. Phys.* **2014**, *16*, 311–323.
- [18] Liu, X.; He, R.; Shen, W.; Li, M. *J. of Mol. Modeling* **2013**, *19*, 4283–4291.
- [19] Zhang, L.; Pei, K.; Yu, M.; Huang, Y.; Zhao, H.; Zeng, M.; Wang, Y.; Gao, J. *J. Phys. Chem. C* **2012**, *116*, 26154–26161.
- [20] Zanlorenzi, C.; Akcelrud, L. *J. Polym. Sci. Part B: Polym. Phys.* **2017**, *55*, 919–927.
- [21] Engel, G. S.; Calhoun, T. R.; Read, E. L.; Ahn, T. K.; Mancal, T.; Cheng, Y. C.; Blankenship, R. E.; Fleming, G. R. *Nature* **2007**,

446, 782–786.

[22] Bittner, E. R.; Kelly, A. *Phys. Chem. Chem. Phys.* **2015**, *17*, 28853–28859.

[23] Moses, D. *Nat. Mat.* **2014**, *13*, 4–5.

[24] Kaake, L. G.; Moses, D.; Heeger, A. J. *J. Phys. Chem. Lett.* **2013**, *4*, 2264–2268.

[25] Ari, M.; Kanat, Z.; Dincer, H. *Solar Energy* 2016, 1–8.

[26] Meng, L.; Zhang, Y.; Wan, X.; Li, C.; Zhang, X.; Wang, Y.; Ke, X.; Xiao, Z.; Ding, L.; Xia, R.; Yip, H.-L.; Cao, Y.; Chen, Y. *Science* **2018**, *361*, 1094–1098.

[27] Yost, S. R.; Hontz, E.; Yeganeh, S.; Van Voorhis, T. *The Journal of Physical Chemistry C* **2012**, *116*, 17369–17377.

[28] Schilinsky, P.; Waldauf, C.; Brabec, C. *J. Appl. Phys. Lett.* **2002**, *81*, 3885–3887.

[29] Mihailetchi, V. D.; Koster, L. J. A.; Humellen, J. C.; Blom, P. W. M. *Phys. Rev. Lett.* **2004**, *93*, 216601.

[30] ASTM G173-03(2012), Standard Tables for Reference Solar Spectral Irradiances: Direct Normal and Hemispherical on 37 Tilted Surface. ASTM International, West Conshohocken, PA, 2012, www.astm.org.

[31] Alharbi, F. H.; Rashkeev, S. N.; El-Mellouhi, F.; Lüthi, H. P.; Tabet, N.; Kais, S. *NPJ Comp. Mat.* 2015, *15003*, 1–9.

[32] Vandewal, K.; Tvingstedt, K.; Gadisa, A.; Inganäs, O.; Manca, J. V. *Nat Mater* **2009**, *8*, 904–909.

[33] Few, S.; Frost, J. M.; Nelson, J. *Phys. Chem. Chem. Phys.* **2015**, *17*, 2311–2325.

[34] Grancini, G.; Maiuri, M.; Fazzi, D.; Petrozza, A.; Egelhaaf, H.-J.; Brida, D.; Cerullo, G.; Lanzani, G. *Nat. Mat.* **2013**, *12*, 29–33.

[35] Grancini, G.; Binda, M.; Criante, L.; Perissinotto, M.; Maiuri, M.; Fazzi, D.; Petrozza, A.; Egelhaaf, H.-J.; Brida, D.; Cerullo, G.; Lanzani, G. *Nat. Mat.* **2013**, *12*, 594–595.

[36] Scharber, M. C. *Advanced Materials* 2016, *28*, 1994–2001.

[37] Tortorella, S.; Talamo, M. M.; Cardone, A.; Pastore, M.; Angelis, F. D. *Journal of Physics: Condensed Matter* **2016**, *28*, 074005.

[38] Becke, A. D. *J. Chem. Phys.* **1993**, *98*, 1372.

[39] Lee, C.; Yang, W.; Parr, R. G. *Phys. Rev. B* **1988**, *37*, 785.

[40] Hachmann, J.; Olivares-Amaya, R.; Atahan-Evrenk, S.; Amador-Bedolla, C.; Sánchez-Carrera, R.; Gold-Parker, A.; Vogt, L.; Brockway, A. M.; Aspuru-Guzik, A. *J. Phys. Chem. Lett.* **2011**, *2*, 2241–2251.

[41] Hachmann, J.; Olivares-Amaya, R.; Jinich, A.; Appleton, A. L.; Blood-Forsythe, M. A.; Seress, L. R.; Román-Salgado, C.; Trepte, K.; Atahan-Evrenk, S.; Er, S.; Shrestha, S.; Mondal, R.; Sokolov, A.; Bao, Z.; Aspuru-Guzik, A. *Energy Environ. Sci.* **2014**, *7*, 698–704.

[42] Li, S.-B.; Duan, Y.-A.; Geng, Y.; Li, H.-B.; Zhang, J.-Z.; Xu, H.-L.; Zhang, M.; Su, Z.-M. *Phys. Chem. Chem. Phys.* **2014**, *16*, 25799–25808.

[43] Ditchfield, R.; Hehre, W. J.; Pople, J. A. *J. Chem. Phys.* **1971**, *54*, 724–728.

[44] Hehre, W. J.; Ditchfield, R.; Pople, J. A. *J. Chem. Phys.* **1972**, *56*, 2257–2261.

[45] Hariharan, P. C.; Pople, J. A. *Theor. Chim. Acta* **1973**, *28*, 213–222.

[46] Gordon, M. S.; Binkley, J. S.; Pople, J. A.; Pietro, W. J.; Hehre, W. J. *J. Am. Chem. Soc.* **1982**, *104*, 2797–2803.

[47] Francl, M. M.; Pietro, W. J.; Hehre, W. J.; Binkley, J. S.; Gordon, M. S.; DeFrees, D. J.; Pople, J. A. *J. Chem. Phys.* **1982**, *77*,

3654–3665.

[48] Shao, Y. *et al. Mol. Phys.* **2015**, *113*, 184–215.

[49] Frisch, M. J. *et al. Gaussian 03, Revision C.02.* Gaussian, Inc., Wallingford, CT, 2004.

[50] Becke, A. D. *J. Chem. Phys.* **1993**, *98*, 1372–1377.

[51] Clark, T.; Chandrasekhar, J.; Spitznagel, G. W.; Schleyer, P. V. R. *J. Comput. Chem.* **1983**, *4*, 294–301.

[52] Krishnan, R.; Binkley, J. S.; Seeger, R.; Pople, J. A. *J. Chem. Phys.* **1980**, *72*, 650–654.

[53] McLean, A. D.; Chandler, G. S. *J. Chem. Phys.* **1980**, *72*, 5639–5648.

[54] Stewart, J. J. P. *J. Comp. Chem.* **1989**, *10*, 209–220.

[55] Spartan 16 Wavefunction, Inc., Irvine, CA.

[56] Meier, H. *Angew. Chem. Int. Ed.* **2005**, *44*, 2482–2506.

[57] Varkey, E. C.; Hutter, J.; Limacher, P. A.; Lüthi, H. P. *J. Org. Chem.* **2013**, *78*, 12681–12689.

[58] Turan, H. T.; Kucur, O.; Kahraman, B.; Salman, S.; Aviyente, V. *Phys. Chem. Chem. Phys.* **2018**, *20*, 3581–3591.

[59] Forberich, K.; Guo, F.; Bronnbauer, C.; Brabec, C. *Energy Tech.* **2015**, *3*, 1051–1058.